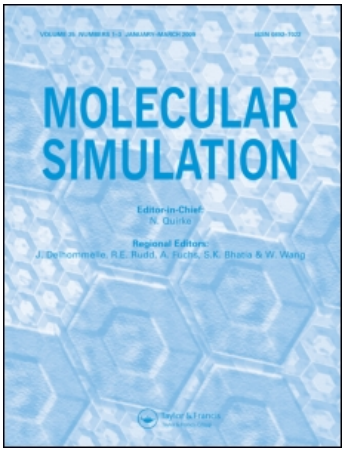

Molecular Simulation
Publication details, including instructions for authors and subscription information:
http://www.informaworld.com/smpp/title~content=t713644482

Dependence of self-diffusivity on size of impurity atoms in a face-centred cubic solid: existence of an anomalous maximum

Chaitanya Krishna[a]; S. Yashonath[abc]
[a] Solid State and Structural Chemistry Unit, Indian Institute of Science, Bangalore, India [b] Center for Condensed Matter Theory, Indian Institute of Science, Bangalore, India [c] Jawaharlal Nehru Centre for Advanced Scientific Research, Jakkur, Bangalore, India

First published on: 21 September 2010

To cite this Article Krishna, Chaitanya and Yashonath, S.(2009) 'Dependence of self-diffusivity on size of impurity atoms in a face-centred cubic solid: existence of an anomalous maximum', Molecular Simulation, 35: 1, 151 — 161, First published on: 21 September 2010 (iFirst)
To link to this Article: DOI: 10.1080/08927020802419342
URL: http://dx.doi.org/10.1080/08927020802419342

Molecular Simulation
Vol. 35, Nos. 1–2, January–February 2009, 151–161

Taylor & Francis
Taylor & Francis Group

Dependence of self-diffusivity on size of impurity atoms in a face-centred cubic solid: existence of an anomalous maximum

Chaitanya Krishna[a] and S. Yashonath[abc]*

[a]*Solid State and Structural Chemistry Unit, Indian Institute of Science, Bangalore, India;* [b]*Center for Condensed Matter Theory, Indian Institute of Science, Bangalore, India;* [c]*Jawaharlal Nehru Centre for Advanced Scientific Research, Jakkur, Bangalore, India*

(*Received 8 July 2008; final version received 18 August 2008*)

Molecular dynamics simulation of a solid solution consisting of smaller impurity or solute atoms within a face-centred cubic lattice of larger solvent atoms is reported at a fixed concentration. Dependence of self-diffusivity of the solute atom on the diameter of the solute has been obtained. The self-diffusivity of the solute exhibits an anomalous maximum. This surprising result is explained in terms of the mutual cancellation of forces when the size of the impurity atom is comparable to the neck diameter present in the face-centred lattice. As interactions among different solids can vary widely, here we report studies employing the van der Waals interactions, which are most ubiquitous of all. Our results suggest that the only condition for the existence of a maximum is the presence of these dispersions or van der Waals interactions. Apart from the fact that these results suggest the existence of a size-dependent diffusivity maximum, they unambiguously indicate that a larger solute does not necessarily diffuse more slowly than a smaller sized solute. These are of significance in metallurgy as well as materials science. The results suggest that there will be situations where heterodiffusion of smaller impurity atoms such as H, B, C, N and O present in interstitials in a typical solid of transition or other elements of larger size can exhibit surprisingly large self-diffusivities under suitable conditions.

Keywords: diffusion; f.c.c. solid; size dependence

1. Introduction

Diffusion in solids has been widely investigated to understand the mechanism, rate, dependence on temperature, etc. The process of diffusion varies with the nature of the diffusive species (termed the solute) and the nature of the host (or solvent) in which it is diffusing. Diffusion of an atom in close-packed solids made up of similar atoms (e.g. self-diffusion in pure metals) proceeds by vacancy diffusion. Atoms diffuse through jumps from one vacant lattice site to another. These have been studied in some detail and are reasonably well understood. The diffusion rates are generally significantly low. As opposed to this, impurity diffusion in pure metals consisting of diffusion of small solutes in close-packed solids made up of atoms of a larger size is found to proceed through jumps from one interstitial site to another. These have also been investigated well and theories as well as experimental investigations on these systems have been discussed in some detail in the literature [1–3].

Diffusion in solids plays an important role in a number of processes such as corrosion, alloy formation and determines a number of properties of the materials such as their strength, resistance to chemical attacks, etc. In metallurgy, for example, diffusion has been studied over many years to understand the properties of different materials.

In the case of diffusion in pure metals where the diffusing species is of smaller size when compared with the atoms defining the lattice, the size of the impurity atom can vary over a wide range. The migration of interstitial solutes such as H, B, C, N and O dissolved in Fe, for example, is important for steel. Similarly, diffusion within other transition elements is important in metallurgical industries. Diffusion within uranium or other radioactive elements is of importance in nuclear waste disposal. In all of these systems, the host element can exist in face-centred, body-centred cubic, as well as simple cubic arrangements. Diffusion of the impurity atoms within these host elements (typically transition elements) is of considerable interest in many industries including the steel industry. The self-diffusivity of the impurity atom determines many of the properties of the transition metal alloys. Often the solvent atom need not be a transition metal. Instead, it could be any other element sufficiently large in size relative to the impurity or solute atom so that the impurity can be accommodated in an interstitial site. Often, the impurity concentration is low and solute–solute interaction is unimportant. A typical example is that of diffusion of H atoms in Pd, which has been well studied [4,5].

In solutions or liquids, the Stokes–Einstein relationship gives a reciprocal dependence of the self-diffusivity

*Corresponding author. Email: yashonath@sscu.iisc.ernet.in

ISSN 0892-7022 print/ISSN 1029-0435 online

DOI: 10.1080/08927020802419342
http://www.informaworld.com

on the size of the solute. The Stokes–Einstein relationship can be given as

$$D = \frac{RT}{N_A} \frac{1}{6\pi\eta r_u}, \quad (1)$$

where r_u is the solute radius, η is the viscosity of the solution, R is the gas constant, N_A is the Avogadro number and T is the temperature, which is valid for solutes of relatively larger size; solute sizes should be similar to the size of the solvent. Recently, we have shown that this relationship breaks down when the solute size is 1/4 the size of the solvent [6]. Furthermore, this breakdown was found to be due to the presence of dispersion interaction between the solute and the solvent.

A systematic study of the dependence of self-diffusivity of the impurity atom on its (solute) radius in different close-packed lattices is (to the best of our knowledge) lacking. It is interesting to see the dependence of the self-diffusivity on the size or diameter of the impurity atom in the light of the above results in binary liquid solutions. Here, we investigate the dependence of the self-diffusivity on the size of the solute or impurity atom. We attempt to answer this by carrying out molecular dynamics simulation of a system consisting of impurity atoms in a face-centred lattice of solvent atoms. Interactions between the solute and the solvent atoms as well as others are chosen to be simple (6-12) Lennard-Jones interaction. In metals, the interactions are admittedly more complex [7,8]. However, to keep the system being investigated as simple as possible and to demonstrate the basic principle that leads to the diffusivity maximum as a function of the diameter of the impurity atom or diffusant, we have chosen to study a system interacting exclusively via the Lennard-Jones potential. Furthermore, dispersion interaction is one of the interactions that exist even in metals. Rare gas solids that have a face-centred cubic arrangement provide one class of systems where the results of the present study will be directly relevant.

The size of the impurity atom is varied and the self-diffusivity is computed from molecular dynamics simulation in the microcanonical ensemble. The results obtained have implications on the diffusion of real atoms and molecules within the face-centred cubic solids.

2. Methods

2.1 Intermolecular potential and molecular dynamics simulations

We have employed the (6-12) Lennard-Jones potential for interactions between the solute–solute, solute–solvent and solvent–solvent atoms. Both the solute and solvent (indicated by subscripts u and v, respectively) are spherical atomic particles with a single interaction site. We assume that these interactions are pairwise additive and the total energy of the system is given by the sum of solute–solute, solute–solvent and solvent–solvent pair interactions. The potential parameters employed in the present study are listed in Table 1. The Lennard-Jones parameter σ_{uu} has been varied between 0.3 and 1.6 Å. Here, we use the same combination rules that have been previously employed in the simulation of simple liquid solutions [9]; the Lennard-Jones parameters for the solute–solvent interactions have been obtained from $\sigma_{uv} = \sigma_{uu} + 0.7$ Å while $\varepsilon_{uv} = 1.5$ kJ/mol for all the runs irrespective of the value of σ_{uv}. Note that there are many systems where the Lorentz–Berthelot rules are not obeyed (e.g. AgI).

Table 1. The solute–solute(uu), solute–solvent(uv) and solvent–solvent(vv) Lennard-Jones interaction parameters.

Type of interaction	ϵ (kJ mole^{-1})	σ (Å)
uu	0.99	0.3–1.6
uv	1.50	$\sigma_{uu} + 0.7$
vv	1.84	4.1

All simulation runs have been carried out in the microcanonical ensemble with spherical cut-off and periodic boundary conditions with the help of DLPOLY package [10]. The molecular dynamics integration was carried out with Verlet leapfrog algorithm. We have kept the composition of the solid solution at 10% in all the runs. Both the impurity and host atoms are included in the molecular dynamics integration.

2.2 Voronoi polyhedra analysis

Although within a face-centred cubic lattice the presence of tetrahedral and octahedral voids and their sizes and interconnectivity has been well understood, since the present simulation provides for the significant movement of the atoms of the host lattice, we prefer to characterise it with the help of Voronoi polyhedral analysis. This method is used to understand the structure of the voids in the studies of liquids [11,12], and other disordered materials such as porous media and powders [13,14], resulting in valuable insights into the distribution of voids within these dense systems.

Briefly, in any specified configuration of equi-sized particles, the Voronoi polyhedron of a given particle i is the set (sub-volume) of all points that are closer to i than to any other. The vertices and edges of the Voronoi polyhedra are, by construction, equally far from the closest surrounding particles. Specifically, in disordered configurations, a Voronoi vertex is equidistant from four particles and any point on the Voronoi edge is equidistant from three particles. Therefore, a natural and convenient description of the empty or void space can be given in terms of the network formed by the edges of the Voronoi polyhedra. Specifically, one can visualise the void space as made

of 'pores', each of radius given by the distance of a Voronoi vertex to the surrounding particles minus the particle radius, and 'channels' of radius given by the smallest lateral distance of a Voronoi edge and the surrounding particles minus the particle radius. We refer to the corresponding diameters as void and neck sizes, respectively.

Diffusants of a given radius can find an interconnected path between voids if the intervening neck sizes are larger than the diffusant radius. However, the motion of the host atoms ensures that the void network is restructured dynamically. In the case of a solid, this is largely limited to small variations in void and neck diameters. Thus, in a liquid, even a solute or a guest particle, for which there is no interconnected path at a given time step, manages to diffuse over a period of time.

Voronoi and Delaunay tessellations have been carried out using the algorithm by Tanemura et al. [15], as outlined in Sastry et al. [12]. The main purpose of the Voronoi analysis is to obtain the distribution of void and neck diameters. For diffusion within perfect crystalline porous solids, the anomalous maximum in the self-diffusivity occurs when the solute radius is nearly the same as the neck radius [16,17]. For diffusion within disordered solids such as the present system [18], the maximum occurs for solute radius less than the most probable neck radius.

3. Computational details

Calculations have been carried out for 14 different Lennard-Jones diameters of the solute: σ_{uu} has been varied between 0.3 and 1.6 Å in intervals of 0.1 Å. Simulations have been carried out on a system of 500 solvent atoms and 50 solute or impurity atoms. The solute species were initially placed at the centres of octahedral or tetrahedral voids within the face-centred cubic structure whose positions were determined from the Voronoi tessellation described above. Both the host and guest atoms are included in the molecular dynamics integration in the microcanonical ensemble. System consists of $5 \times 5 \times 5$ face-centred solvent or host lattice with a lattice parameter of 6.66 Å. Molecular dynamics simulations have been carried out at 50 K, corresponding to the reduced temperature: $T* = 0.226$. A time step of 5.0 fs is found to have good energy conservation (1 in 10^4). Equilibration is over 1.0 ns and averages are accumulated over an equal period. Positions and velocities are stored every 0.25 ps for further analysis. Calculation of the void and neck distributions has been carried out using 400 of these configurations. Other properties were averaged over all the stored configurations above 1 ns. Simulations were performed in a cubic cell of length 33.3 Å with a cut-off radius of 16.5 Å. The density considering only the solvent atoms is $\rho* = 0.933$. All properties indicated by asterisks are in reduced units that are expressed in terms of interaction parameters for vv interaction ($\varepsilon_{vv} = 1.84$ kJ/mol and $\sigma_{vv} = 4.1$ Å).

4. Results and discussion

4.1 Structural properties

Solvent–solvent radial distribution function (rdf) for 4 solute diameters out of the 14 for which simulations have been carried out are shown in Figure 1(a). There is no noticeable difference in the solvent–solvent rdf when the solute size is varied. As expected, the solvent remains mostly in a well-defined face-centred solid at $T* = 0.226$. The solvent motion is largely confined to vibrational motion around the equilibrium sites, which is what one expects at $T* = 0.226$. This is also evident from the snapshot (Figure 1(c)) that clearly shows the existence of well-defined planes that will yield diffraction patterns of a f.c.c. solid.

The solute–solvent rdf is shown in Figure 1(b). As can be seen, there is a decrease in the height of the first peak from 0.3 to 1.1 Å. An increase in the peak height is seen for sizes larger than 1.1 Å. It can be seen later that the peak height is related inversely to mobility as well as liquid-like behaviour.

The distribution ($g(d*)$) of the void and neck diameters $d* = d/\sigma_{vv}$ have been computed from the Voronoi analysis, and is shown in Figure 1(d). There are no significant differences in the distribution of the void and neck for different sizes of the solute. The neck distribution peaks at a lower value of $d*$, where $d*$ is the diameter of the void or neck. A bimodal distribution of voids is shown in Figure 1(d). The void size distribution of the disordered f.c.c. crystal exhibits two peaks at void sizes of $d* \simeq 0.35$ and 0.55. This is in agreement with the previously calculated void distribution for a f.c.c. solid by Corti et al. [11]. The peaks at $d* = 0.35$ and 0.55 correspond to the tetrahedral and octahedral voids, respectively [19], in the f.c.c. crystal. Note that the characteristic double peak in the void size distribution was also seen by Finney and Wallace [20] in a study of random packing of soft spheres.

As we show below, an understanding of the changes in the solute–solvent rdfs requires a knowledge of the dynamical properties.

4.2 Dynamical properties

4.2.1 Dependence of self-diffusivity on the size of the impurity atom

The time evolution of the mean square displacement (m.s.d.) and $u^2(t)$ of solute and the solvent at 50 K is shown in Figure 2 for different solute sizes. The self-diffusivities have been computed from the slope of the m.s.d. These values are listed in Table 2. Figure 3 shows two sample trajectories over 200 ps, along with the host

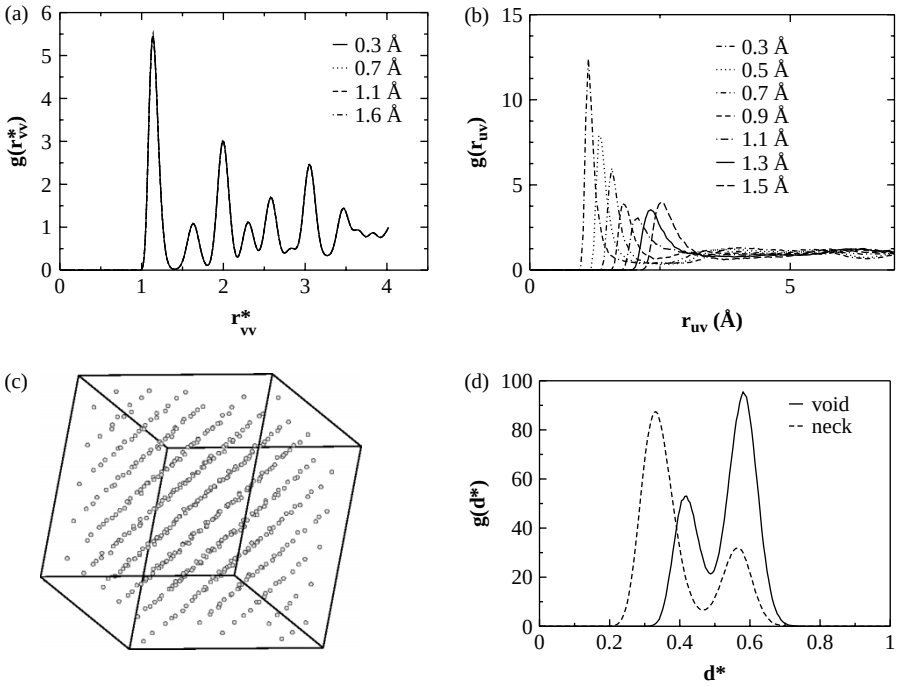

Figure 1. (a) Solvent–solvent rdf ($r^*_{vv} = r_{vv}/\sigma_{vv}$). (b) Solvent–solute rdf. (c) A view of the final f.c.c. structure showing the presence of distinct planes. (d) Void and neck distribution ($d^* = d/\sigma_{vv}$).

lattice. The trajectory of the linear regime (LR) particle of 0.7 Å size is shown by the smaller sized atoms and the anomalous regime (AR) particle of 1.1 Å size is shown by the larger sized trajectory. The equilibrium positions of the host lattice are also shown. The AR particle is seen to traverse over a significantly longer distance when compared with LR over the 200 ps.

Self-diffusivities are plotted in Figure 4 against reciprocal of the square of the solute diameter, $1/\sigma^2_{uu}$. For small values of σ_{uu}, the relationship $D \propto 1/\sigma^2_{uu}$, expected on the basis of kinetic theory, is seen to be valid. For large values of σ_{uu}, we see that the self-diffusivity increases with the size of the impurity atom, instead of a decrease seen in the LR. This leads to a maximum in the self-diffusivity. For still a larger size of the impurity atom, D subsequently decreases. These both are referred to as the AR.

Although the solvent atoms are mobile, the diffusivity of the solvent is very small (of the order of 10 m/s

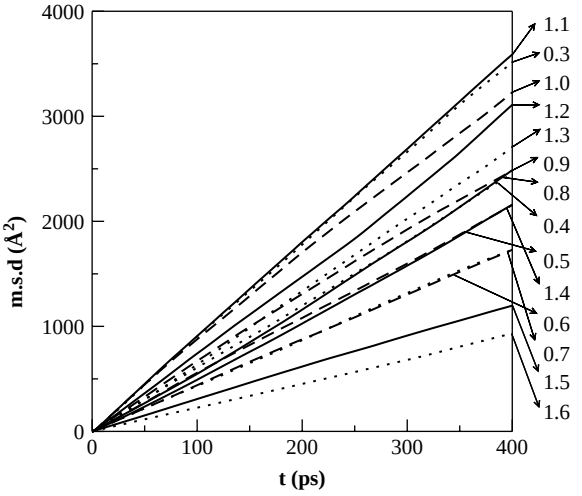

Figure 2. Mean square displacement of different sized solutes (in Å).

Table 2. Self-diffusivity of the impurity or solute atoms at 50 K as a function of the size of the impurity atom, σ_{uu}, in a face-centred cubic lattice. Solvent diffusivity is significantly smaller (10^{-12} m^2/s).

σ_{uu} (Å)	D (10^{-8} m^2/s)
0.3	1.48
0.4	1.01
0.5	0.87
0.6	0.72
0.7	0.74
0.8	1.05
0.9	1.04
1.0	1.33
1.1	1.49
1.2	1.19
1.3	1.15
1.4	0.91
1.5	0.50
1.6	0.38

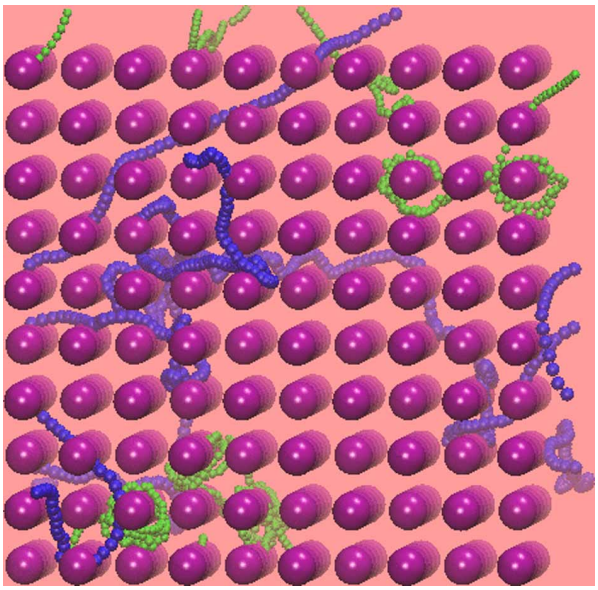

Figure 3. Trajectory of the LR (size 0.7 Å, green) and AR (size 1.1 Å, blue) impurity atoms in 5 × 5 × 5 face-centred lattice (purple) over 200 ps, showing that the former traverses over not as long a distance as the latter particle due to significant localised motion. For purposes of display, the Lennard-Jones diameter of host atoms has reduced from 4.1 Å employed in the MD simulation to 2.6 Å. This gives a more clear view of the trajectory of the linear and anomalous impurity atoms.

or smaller). This may be compared with the solute diffusivity of about 10 m/s. Solvent essentially undergoes vibrational motion around its equilibrium position and no long-range diffusional motion on the time scale of the simulation.

A dimensionless parameter is defined as

$$\gamma = \frac{\sigma_{\text{opt}}}{\sigma_{\text{w}}},$$

where σ_{opt} is the distance at which the interaction between the diffusant and the medium (through which it is diffusing) is optimum and σ_{w} is the neck diameter. The neck diameter is the narrowest part of the void that the diffusant encounters along its diffusion path. γ is called the Levitation parameter because when this is close to unity, the force exerted on the diffusant by the atoms of the medium in which the diffusant is placed is the lowest and the diffusant 'levitates' in this sense, leading to higher self-diffusivity. σ_{opt} is the distance at which the interaction between the solute and the host atoms are optimum; by optimum we mean that the interaction energy is large and negative. For the Lennard-Jones potential, this occurs at a distance of 2σ. Figure 5 shows a plot of D against γ. For diffusion in ordered systems such as when the crystalline lattice is static or rigid, an example of which is guest diffusion in rigid zeolite lattice, the maximum in D is seen for γ close to unity. However, when host lattice is dynamic possessing good degree of disorder as in the present case, the void and neck diameters are not unique and have a broad distribution, then the maximum in D is seen for γ significantly less than unity [18]. In the present study, we note that the displacements in the equilibrium positions of the solvent atoms are significant compared with the distance between them: thus from the solvent–solvent rdf (Figure 1(a)), we see that the nearest neighbour distance is around 4.5 Å and the spread of the first peak extends over a distance of 1.6 Å. Thus, the amplitude of vibration is about 0.33 times the nearest neighbour distance. The large motion of the solvent leads to the presence of significant degree of disorder leading to the maximum in self-diffusivity at a much lower value of γ.

In order to understand the nature of the observed maximum in self-diffusivity, we have computed a number

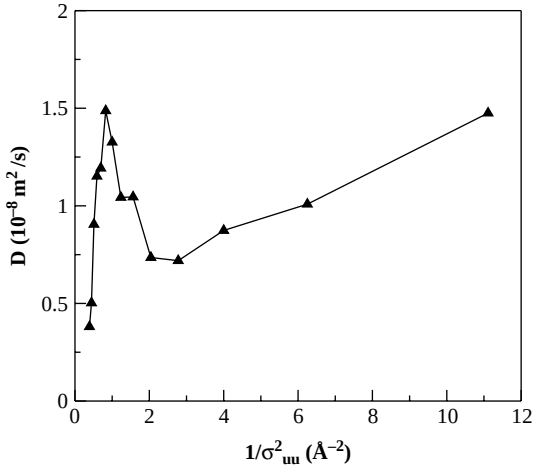

Figure 4. Self-diffusivity D against reciprocal of the square of the solute diameter.

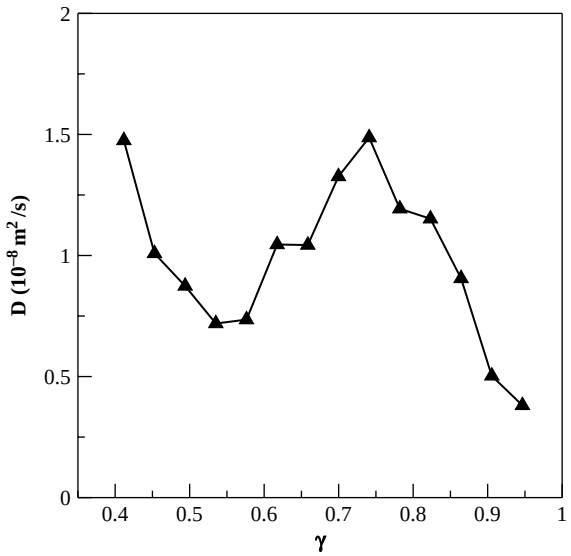

Figure 5. Variation in self-diffusivity D with the levitation parameter γ.

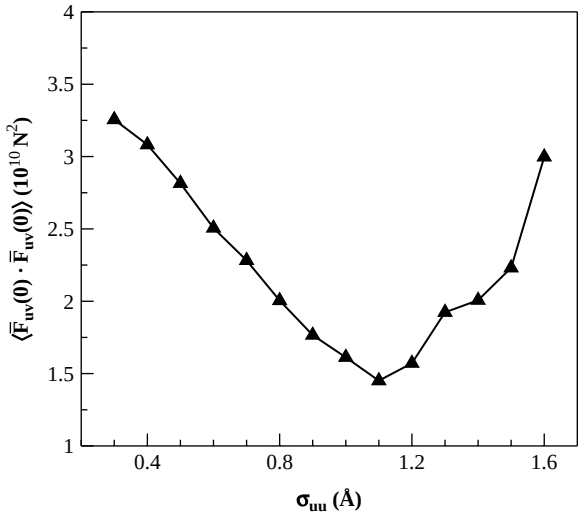

Figure 6. The dependence of average force squared, $F_{uv}(0) \cdot F_{uv}(0)$, on the size of the guest. The quantity has been obtained by averaging over all times and solutes.

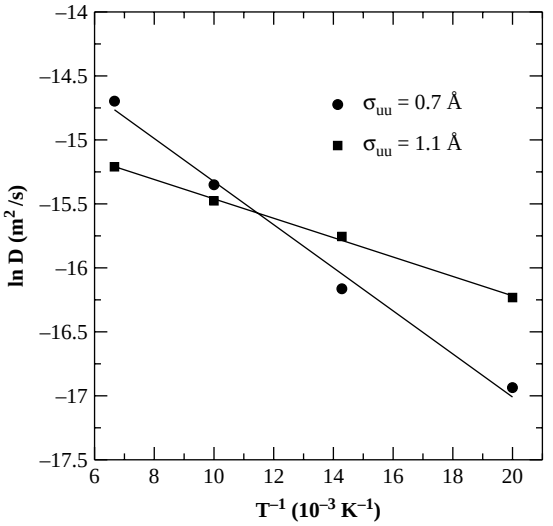

Figure 7. Arrhenius plot of self-diffusivity for a particle from LR ($\sigma_{uu} = 0.7$ Å) and AR ($\sigma_{uu} = 1.1$ Å). Note the lower activation energy for the particle from the AR suggesting that the observed maximum in D arises from the LE.

of properties. In Figure 6, we show the variation in the average force squared on the solute arising from the surrounding solvent lattice as a function of the size of the solute. The force squared has been averaged over all simulation times and solutes. This quantity is nothing but the zero time limit of the force autocorrelation function, $F_{uv}(0) \cdot F_{uv}(0)$. Note that the average force squared decreases with increase in the size of the solute, eventually reaching a minimum for the size of the solute, $\sigma_{uu} = 1.1$ Å, for which self-diffusivity is a maximum. The average force on the solute due to the solvent increases with the increase in the size beyond 1.1 Å.

4.2.2 *Activation energies in linear and ARs*

Table 3 lists the values of self-diffusivity at four different temperatures for $\sigma_{uu} = 0.7$ Å and $\sigma_{uu} = 1.1$ Å. Figure 7 shows the Arrhenius plot of the self-diffusivity D. Activation energies have been calculated from the slope of the straight line obtained from a least squares fit to the data. The values of activation energies for 0.7 Å particle is 1.4 kJ/mol. For 1.1 Å particle, $E_a = 0.77$ kJ/mol.

The solute–solvent interaction energy for a guest particle during the migration (or jump) from one void to another was computed as a function of the perpendicular distance from the plane bisecting the line joining the two void centers. This distance can be considered to be the diffusion coordinate. The solute–solvent energy yields the potential energy landscape that the guest encounters before and after a jump from one void to another. Figure 8 shows the potential energy landscape for guest sizes

Table 3. Self-diffusivity values at different temperatures for two different guest sizes, one from LR and another from AR.

Temperature (K)	D ($\sigma_{uu} = 0.7$ Å; 10^{-8} m^2/s)	D ($\sigma_{uu} = 1.1$ Å; 10^{-8} m^2/s)
50	4.41	8.92
70	9.55	14.38
100	21.55	19.00
150	41.44	24.79

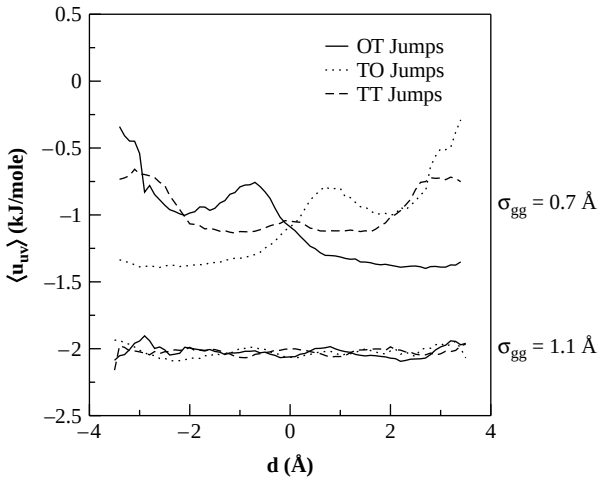

Figure 8. Variation in the potential energy landscape with the perpendicular distance of the impurity atom from the plane bisecting the line joining the two neighbouring voids (one in which the diffusing atom is located and the neighbouring void into which it jumps) for the LR ($\sigma_{uu} = 0.7$ Å) and AR ($\sigma_{uu} = 1.1$ Å) particles. We present the results for three different jumps: jump from an OT void, TO void and TT void at 50 K. These have been obtained by first listing all jumps from one void to another and then classifying them into different categories (TT, OT or TO) and averaging the potential energy profile over all jump events of that particular category.

Table 4. Jump frequencies in units of 10^{11} jumps per guest per second for OO, OT, TO and TT jumps obtained by averaging over all solutes and over 500 ps.

Solute size (Å)	Jump type				
	OO	OT	TO	TT	Total
0.7	0.0000	3.1472	3.1468	2.4124	8.0706
1.1	0.0000	2.0988	2.1040	3.4008	7.6036

$\sigma_{uu} = 0.7$ Å and $\sigma_{uu} = 1.1$ Å corresponding to the linear and the ARs, respectively, at 50 K for different kinds of jumps: octahedral to tetrahedral (OT), tetrahedral to octahedral (TO), etc. The interaction energy was computed for a total of 500 ps with the configurations stored every 0.01 ps. The jump frequencies for both the LR and AR particles are given in Table 4. It is interesting to note that there are no jumps from an octahedral to octahedral void, possibly because of the steep potential the solute particle encounters (not shown) before it can go to the next octahedral void. The plot clearly illustrates that the potential energy surface for the AR particle is much shallower than that of the LR particle and devoid of significant energy barriers.

The velocity autocorrelation function $c(t)$ is shown in Figure 9 for different sizes of the solutes. It can be seen that the particle in the LR (e.g. $\sigma_{uu} = 0.7$ Å) exhibits a significant negative correlation, which is absent for the larger particle in the AR (e.g. $\sigma_{uu} = 1.1$ Å).

4.2.3 *Wavevector-dependent self-diffusivity*

Dependence of self-diffusivity on wavevector k where $k = 2\pi n/L$ can yield valuable information about the mechanism of diffusion. Here L is the simulation cell length and n are non-zero positive integers. In the hydrodynamic limit ($k \rightarrow 0, \omega \rightarrow 0$), the simple diffusion model is valid and the full width at half maximum, $\Delta\omega$ of the dynamic structure factor $S_s(k,\omega)$, is proportional to $2Dk^2$. As is well known, the motion in the intermediate range of k values is strongly influenced by the intermolecular potential. We have computed the $\Delta\omega(k)$ in the intermediate k region for a particle from the linear and the ARs. Note that $\Delta\omega(k)$ is the full width at half maximum of the self-part of $S_s(k,\omega)$. It provides an estimate of the magnitude of the self-diffusivity, $\Delta\omega(k) \propto D(k)$. Dynamic structure factor, $S_s(k,\omega)$, was obtained from the Fourier transform of the intermediate scattering function $F_s(k,t)$ for several sizes of the guest. $F_s(k,t)$ was computed by taking a powder average [21].

Previously, Nijboer and Rahman [22] as well as Levesque and Verlet [23] have investigated the variation in the ratio $\eta(k) = \Delta\omega/2Dk^2$ with k for argon. They have investigated the variation in $\eta(k)$ for two thermodynamic states: $\rho* = 0.8442$, $T* = 0.722$, a high-density fluid at low temperature [22] and $\rho* = 0.65$, $T* = 1.872$, a fluid

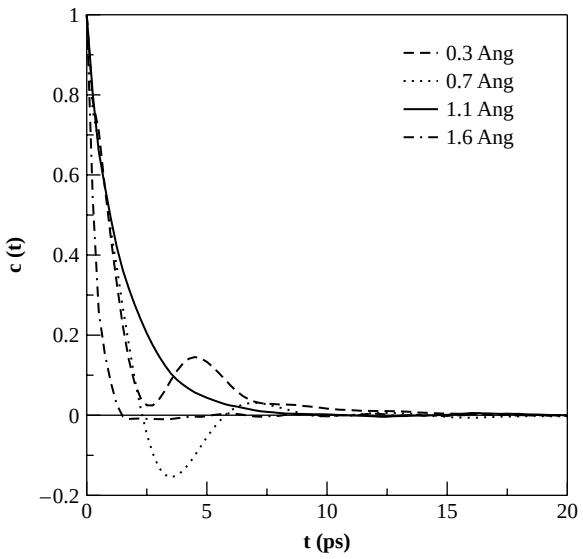

Figure 9. Velocity autocorrelation function for the solute or impurity atoms of size $\sigma_{uu} = 0.3$, 0.7 Å from the LR and $\sigma_{uu} = 1.1$, 1.6 Å from the AR.

at low density at high temperature [23]. Nijboer and Rahman [22] found that the variation in $\Delta\omega(k)/2Dk^2$ for high density fluid at low temperature ($\rho* = 0.8442$, $T* = 0.722$) exhibits a minimum and a maximum. The minimum in $\Delta\omega(k)$ was found to correspond to the k value at which strong correlations are seen in the static structure factor $S(k)$. This probably suggests that the diffusing species has a lower self-diffusivity at around the first and second shells although this needs to be established unambiguously. By contrast, for the low-density, high-temperature fluid which Levesque and Verlet [23] investigated, $\Delta\omega(k)/2Dk^2$ decreased monotonically with k. In this case, it appears that the low density leads to no lowering of diffusion rate at intermediate k. The spatial correlations are largely weakened at this density and no well-defined first and second shell neighbours exist. Thus, the behaviour of $\Delta\omega(k)/2Dk^2$ provides interesting insight into the rate of diffusion near the first shell of neighbours.

Figure 10 shows the variation in $\Delta\omega(k)/2Dk^2$ with k for $\sigma_{uu} = 0.7$ Å (from LR) and $\sigma_{uu} = 1.1$ Å (from AR). For $\sigma_{uu} = 0.7$ Å, a minimum and a maximum are seen as k increases. By contrast, for $\sigma_{uu} = 1.1$ Å, a monotonic decrease with k is seen. Our calculations are for a density of $\rho* = 0.933$. This is higher than that of Nijboer and Rahman [22] ($\rho = 0.8442$), and at such high densities one expects a minimum in $\Delta\omega(k)/2Dk^2$. Thus, the behaviour of the particles in LR (e.g. $\sigma_{uu} = 0.7$ Å) is understandable. However, the larger solutes in the AR (with $\sigma_{uu} = 1.1$ Å) are able to diffuse unimpeded by the spatial correlations even in a close-packed solid without encountering any barrier. This is because of the symmetry encountered by the guest when its size is comparable to the neck diameter. This leads to mutual cancellation of forces exerted by the

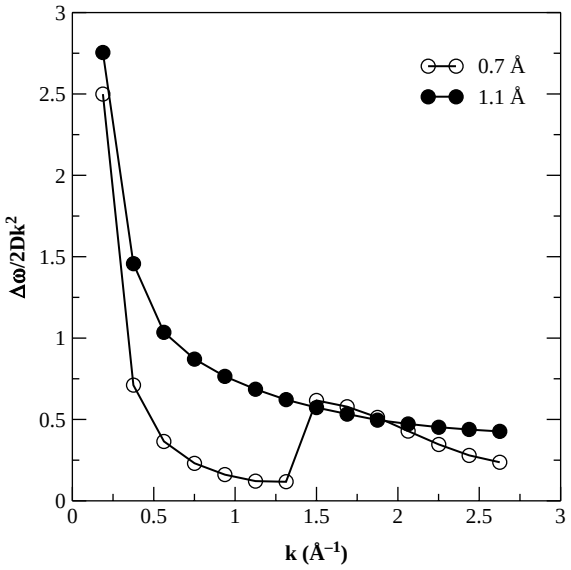

Figure 10. $\Delta\omega(k)/2Dk^2$ as a function of k at 50 K for two LRs and ARs. Note that the AR regime particle exhibits a monotonic decay with k, suggesting no significant slowing down of diffusion at intermediate k values. By contrast, the particle from LR exhibits a non-monotonic decay with the lowest value at around $k = 1.3$ Å when compared with the self-diffusivity in the hydrodynamic limit.

host or solvent on the solute or guest. This is reflected in the lowered force on the solute by the solvent. The dependence of $\Delta\omega(k)/2Dk^2$ for the LR is similar to diffusion within a high-density, low-temperature fluid, while that of the larger sized particle from the AR is similar to diffusion within a low-density, high-temperature fluid! Note that the calculations of both Nijboer and Rahman [22] and Levesque and Verlet [23] are for a single-component fluid consisting of equi-sized Lennard-Jones particles, while in our case there are two components. There are other important differences between the present system and the system of pure argon studied by Nijboer and Rahman as well as Levesque and Verlet. In the present system, the solute in the AR exhibits a strong interaction with the rest of the system (the solvent), while in the case of liquid argon, at low density, high temperature the interactions are weak. The force exerted on the diffusant by the medium (in which the diffusant exists) is lowered in both the solute–solvent and liquid argon. However, the lowered force on the diffusant is due to the decrease in density in the case of liquid argon. In the case of the solute–solvent investigated here, the lowering of the force occurs selectively even at high density for a solute of specific size.

Zeolites Y and A have large cage-like structures (diameter $\simeq 11-12$ Å) interconnected via narrower windows (7.5 Å Y and 4.0 Å in A). In earlier studies on these zeolites with guests of varying sizes, it was found that an energetic barrier exists in the bottleneck for particles from LR [17]. For AR, no such barrier was seen at the window, the bottleneck for diffusion [17]. In the present study on close-packed solids, the narrow necks that interconnect two voids provide the bottlenecks for diffusion. It is well known that the bottleneck for diffusion in the case of face-centred arrangement is of $0.155R$, where R is the radius of the packing spheres (here of the solvent). The similarity in the present case to that of zeolite suggests that the minimum in $\Delta\omega(k)/2Dk^2$ for LR seen at around 1.3 Å could arise from the energetic barrier for getting past the shells of neighbours. A smooth variation in $\Delta\omega(k)/2Dk^2$ with k for the AR particles appears to suggest the absence of such a barrier. At large k, both LR and AR vary as $1/k$ with k. Furthermore, these results are also in agreement with those found for dense liquids [24] where a particle in the LR exhibits a maximum and a minimum in $\Delta\omega(k)/2Dk^2$ while a particle in the AR shows a monotonic decrease in $\Delta\omega(k)/2Dk^2$ with k. Thus, the present calculations suggest that the behaviour in a close-packed solid is, in many ways, similar to the behaviour of a diffusant in a porous solid as well as dense liquids.

The decrease in $\Delta\omega(k)/2Dk^2$ for the particle in the LR and the energetic barrier is likely to lead to well-separated time scales for motion before and past the energy barrier arising from spatial correlations. Decay of $F_s(k,t)$ at intermediate k for the LR particle will therefore exhibit two distinct time scales as it experiences an inhomogeneous environment. Motion at short times is facile, but at long times the motion is slowed down due to the barrier encountered by the LR particle at the neck. For the particle in the AR, absence of such slowing down and any energetic barrier past the first shell is expected to lead to a homogeneous motion

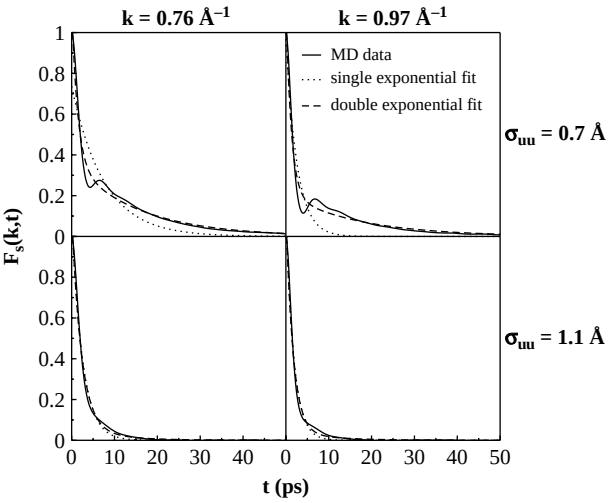

Figure 11. Intermediate scattering function, $F_s(k,t)$ for a typical particle in the LR ($\sigma_{uu} = 0.7$ Å) and AR ($\sigma_{uu} = 1.1$ Å) is shown. Single ($A_1 e^{-t/\tau_1}$) and double exponential ($A_1 e^{-t/\tau_1} + A_2 e^{-t/\tau_2}$) fits are shown. The AR particle fits well to the single exponential but the LR particle fits well only to the double exponential.

Table 5. Values of relaxation times (in ps) derived from the single and biexponential fits to the intermediate scattering function for a typical particle from the LR ($\sigma_{uu} = 0.7$ Å).

	Single		Double			
k (Å^{-1})	A_1	τ_1	A_1	τ_1	A_2	τ_2
0.76	0.74	7.53	0.77	1.39	0.36	15.56
0.97	0.97	2.61	0.94	1.22	0.21	17.05

Note the two widely differing relaxation times associated with a particle from LR.

Table 6. Values of relaxation times (in ps) derived from the single and biexponential fits to the intermediate scattering function for a typical particle from the AR ($\sigma_{uu} = 1.1$ Å).

	Single		Double			
k (Å^{-1})	A_1	τ_1	A_1	τ_1	A_2	τ_2
0.76	1.10	2.49	1.04	2.22	0.07	8.02
0.97	1.10	1.84	1.07	1.68	0.05	8.85

Note that there is a single relaxation time for a particle from AR. This is evident from the small value of A_2 when compared with A_1.

at small k throughout. The signature of these should be seen in the decay of the density fluctuations.

We have calculated the intermediate scattering function, $F_s(k,t)$, for $\sigma_{uu} = 0.7$ Å (LR) and $\sigma_{uu} = 1.1$ Å (AR) particles. Figure 11 shows a plot of $F_s(k,t)$ for $\sigma_{uu} = 0.7$ Å and $\sigma_{uu} = 1.1$ Å for $k = 0.76$ Å and 0.97 Å. To the $F_s(k,t)$, we have fitted single exponential decay ($A_1 e^{-t/\tau_1}$) and double exponential decay ($A_1 e^{-t/\tau_1} + A_2 e^{-t/\tau_2}$) for different k values. As shown in Figure 11, single exponential decay provides a good fit to the $F_s(k,t)$ of the $\sigma_{uu} = 1.1$ Å particle but not to the $\sigma_{uu} = 0.7$ Å particle. For the latter, a double exponential provides a good fit (see Tables 5 and 6). This is consistent with the behaviour of $\Delta\omega(k)/2Dk^2$.

4.3 Physical picture of solute motion

The picture that emerges for the motion of an impurity or solute atom in a face-centered cubic lattice is as follows. A solute particle in the LR diffuses in a facile manner up to a short distance, a distance probably determined by the first shell of solvent neighbours. Diffusion past this first shell of neighbours is not facile. The particle from the LR encounters a distinct energy barrier at probably the first shell of neighbours. Both the potential energy and entropic barriers are expected at the first shell. Once the particle in the LR manages to overcome this barrier and diffuse past the first shell of host neighbours, the solute traverses over a relatively larger distance without difficulty (Figure 12(a)). The relaxation time τ_1 is associated with the motion within the first shell, while τ_2 is associated with the motion past the first shell.

A particle in the LR probably performs an oscillatory motion inside the first shell of neighbours before escaping from it. In other words, the solute is trapped within the first solvent shell of neighbours and performs a vibrational motion since there is an energy barrier for the motion past the first shell. Thus, the first shell provides a cage-like structure in which the guest atom is trapped for a period. For a particle in the AR, no cage-like structure exists. The projection of the trajectory of a particle from the LR ($\sigma_{uu} = 0.7$ Å) and AR ($\sigma_{uu} = 1.1$ Å) is shown in Figure 12(a),(b), respectively. Note that the high-density area exists only for the LR. These have been marked by ellipses with the help of dashed lines. By contrast, the particle from the AR shows no high-density region, suggesting the absence of oscillatory motion of the guest within the first shell of solvent atoms. These trajectories provide evidence in support of our interpretation of the single and biexponential decay of the intermediate

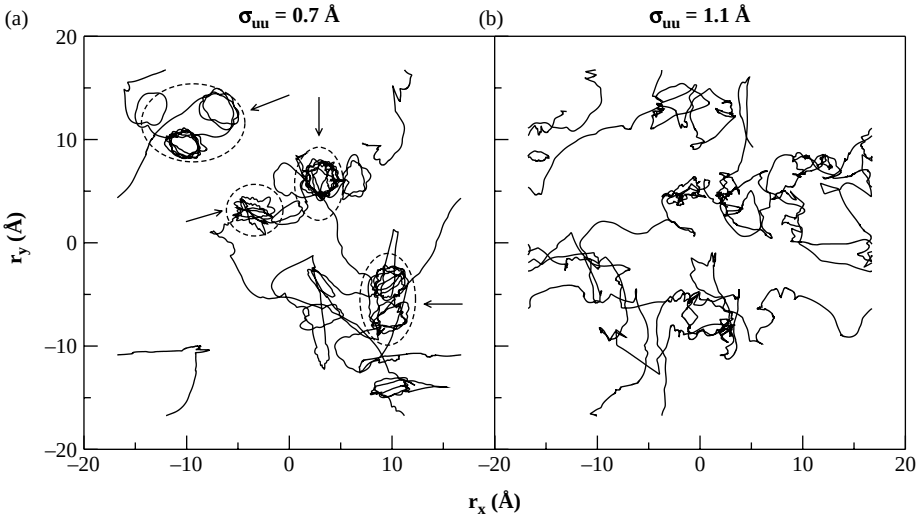

Figure 12. Plot of the projection of the trajectory of a guest particle on to the xy-plane. (a) $\sigma_{uu} = 0.7$ Å (LR). The guest particle oscillates in particular regions that are shown by the dashed ellipses. (b) $\sigma_{uu} = 1.1$ Å (AR). No such behaviour is seen for the particle from the AR. The positions are from configurations stored every 0.01 ps for 500 ps.

scattering function. They also suggest that the interpretation of the variation in $\Delta\omega(k)/2Dk^2$ with k was likely to be correct.

5. Conclusions

In summary, the self-diffusivity of the solute exhibits two distinct regimes: the linear and the AR. There are several characteristics that distinguish the two regimes. (i) The former exhibits a monotonic dependence on the size of the solute; self-diffusivity is seen to decrease with the increase in the size. By contrast, the AR exhibits a non-monotonic dependence of self-diffusivity on the size of the solute. Thus, a maximum in D is seen. (ii) The force on the solute exerted by the solvent or medium is lower for a solute belonging to the AR when compared with the LR. (iii) The velocity autocorrelation function shows little or no backscattering for a solute from the AR. By contrast, a solute from the LR exhibits a pronounced backscattering. (iv) The activation energy is lower for the AR when compared with LR. This is consistent with the less undulating potential energy landscape for a diffusant from the AR seen previously in zeolites, dense liquids and ionic solids [9,17,25]. (v) The intermediate scattering function exhibits a double exponential decay normally. This is what is seen for a solute from the LR. Surprisingly, the intermediate scattering function of a solute from the AR exhibits a single exponential decay. (vi) The full width at half maximum of a particle from the LR exhibits a non-monotonic or oscillatory dependence on wavevector k. This is the normal behaviour. By contrast, the solute belonging to the AR exhibits a monotonic decay with k. Such a monotonic decay is usually seen only in low-density systems. The fact that such a behaviour is seen in dense systems here suggests that the solute is able to diffuse in a facile manner. We attribute this to the absence of a barrier for the diffusion past, probably, the first shell of solvent.

The results here, coupled with previous studies, suggest that the only condition for the existence of the diffusivity maximum or the levitation effect is the presence of dispersion interaction between the solute and the solvent. Furthermore, they also suggest that such a maximum can be seen in the systems with a good degree of order as well as a large degree of disorder. This suggests that such a maximum in self-diffusivity should be seen in other crystalline solids as well. We are presently investigating diffusion in other ordered solids. Previously, we have reported the presence of a maximum for self-diffusivity of an ion in Nasicons [25–27]. The present study suggests that more detailed investigations are necessary to understand the anomalous maximum, especially the reason for the smooth decay of $\Delta\omega(k)/2Dk^2$ with k.

The results here have implications for heterodiffusion where the impurity atoms can diffuse within a face-centred lattice consisting of atoms relatively larger in size. The results suggest that the self-diffusivity of the impurity atom does not vary monotonically with size and that the interaction between the impurity atom and the atoms of the lattice is important. However the fact that atoms come in discrete sizes, it may be difficult to find the correct combination of these three: (a) guest, (b) host and (c) the right density at which the diffusivity maximum will be seen. However, there are non-elemental solids such as Nasicons where the lattice parameter varies as a function of composition where such a maximum is easily observed, since when the lattice parameter varies as a function of composition, there will be an appropriate composition at which the neck diameter will match the diffusant diameter. The present work further suggests that there is an optimum size of the impurity atom for which the diffusivity is maximum and smaller impurity atoms do not necessarily diffuse faster. These might have implications in corrosion, diffusion of atoms such as hydrogen in Pd, etc.

Acknowledgements

We wish to thank the Department of Science and Technology, New Delhi, for financial support.

References

[1] A.R. Allnatt, *Atomic Transport in Solids*, Cambridge University Press, Cambridge, 1993.
[2] A.S. Nowick and J.J. Burton, *Diffusion in Solids: Recent Developments*, Academic Press, London, 1975.
[3] P. Shewmon, *Diffusion in Solids*, McGraw-Hill Book Company, Inc, New York, 1963.
[4] A. Gross and M. Scheffler, Ab initio *quantum and molecular dynamics of the dissociative adsorption of hydrogen on Pd(100)*, Phys. Rev. B 57(4) (1998), pp. 2493–2506.
[5] R.J. Behm, V. Penka, M.G. Cattania, K. Christmann, and G. Ertl, *Evidence for 'subsurface' hydrogen on Pd(110): an intermediate between chemisorbed and dissolved species*, J. Chem. Phys. 78(12) (1982), pp. 7486–7490.
[6] M. Sharma and S. Yashonath, *Breakdown of the Stokes–Einstein relationship: role of interactions in the size dependence of self-diffusivity*, J. Phys. Chem. B 110(34) (2006), pp. 17207–17211.
[7] M. Finnis, *Interatomic forces in materials*, Prog. Mater. Sci. 49(1) (2004), pp. 1–18.
[8] M. Finnis and R. Drautz, *Forward*, Prog. Mater Sci. 52 (2007), pp. 131–132.
[9] P.K. Ghorai and S. Yashonath, *The Stokes–Einstein relationship and the levitation effect: size-dependent diffusion maximum in dense fluids and close-packed disordered solids*, J. Phys. Chem. B 109(12) (2005), pp. 5824–5835.
[10] W. Smith and T.R. Forester, *DL-POLY-2.0: A general-purpose parallel molecular dynamics simulation package*, J. Mol. Graph. 14(3) (1996), pp. 136–141.
[11] D.S. Corti, P.G. Debenedetti, S. Sastry, and F.H. Stillinger, *Constraints, metastability, and inherent structures in liquids*, Phys. Rev. E 55(5) (1997), pp. 5522–5534.
[12] S. Sastry, D.S. Corti, P.G. Debenedetti, and F.H. Stillinger, *Statistical geometry of particle packings. i. Algorithm for exact determination of connectivity, volume, and surface areas of void space in monodisperse and polydisperse sphere packings*, Phys. Rev. E 56 (1997), pp. 5524–5532.
[13] H.L. Weissberg and S. Prager, *Viscous flow through porous media. 2. Approximate 3-point correlation function*, Phys. Fluids 5(11) (1962), pp. 1390–1392.

[14] M. Shahinpoor, *Statistical mechanical considerations on the random packing of granular materials*, Powder Technol. 25(2) (1980), pp. 163–176.
[15] M. Tanemura, T. Ogawa, and N. Ogita, *A algorithm for three-dimensional Voronoi tessellation*, J Comput. Phys. 51(2) (1983), pp. 191–207.
[16] S. Yashonath and P. Santikary, *Diffusion in zeolites: anomalous dependence on sorbate diameter*, J. Chem. Phys. 100(5) (1994), pp. 4013–4016.
[17] S. Yashonath and P. Santikary, *Diffusion of sorbates in zeolites Y and A: novel dependence on sorbate size and strength of sorbate–zeolite interaction*, J. Phys. Chem. 98(25) (1994), pp. 6368–6376.
[18] A.V. Anil Kumar and S. Yashonath, *Effect of a distribution of pore dimension on levitation effect*, J. Phys. Chem. B 104(39) (2000), pp. 9126–9130.
[19] K.J. Laidler and H.J. Meiser, *Physical Chemistry*, Benjamin-Cummings, Reading, MA, 1982.
[20] J.L. Finney and J. Wallace, *Interstice correlation functions – a new, sensitive characterisation of non-crystalline packed structures*, J. Non-Cryst. Solids 49(1) (1981), pp. 165–187.
[21] K.W. Herwig, Z. Wu, P. Dai, H. Taub, and F.Y. Hansen, *Quasielastic neutron scattering and molecular dynamics simulation studies of the melting transition in butane and hexane monolayers adsorbed on graphite*, J. Chem. Phys. 107(13) (1997), pp. 5186–5196.
[22] B.R.A. Nijboer and A. Rahman, *Expansion of correlation functions and theory of slow neutron scattering*, Physica 32(2) (1966), pp. 415–432.
[23] D. Levesque and L. Verlet, *Computer 'experiments' on classical fluids. iii. Time-dependent self-correlation functions*, Phys. Rev. A 2(6) (1970), pp. 2514–2528.
[24] P.K. Ghorai and S. Yashonath, *Levitation effect: distinguishing anomalous from linear regime of guests sorbed in zeolites through the decay of intermediate scattering function and wavevector dependence of self-diffusivity*, J. Phys. Chem. B 109(9) (2005), pp. 3979–3983.
[25] P. Padma Kumar and S. Yashonath, *Ion mobility and levitation effect: anomalous diffusion in Nasicon-type structure*, J. Phys. Chem. B 106(13) (2002), pp. 3443–3448.
[26] P.P. Kumar and S. Yashonath, *A full interionic potential for $Na_{1+x}Zr_2Si_xP_{3-x}O_{12}$ superionic conductors*, J. Amer. Chem. Soc. 124(15) (2002), pp. 3828–3829.
[27] P. Kumar and S. Yashonath, *Structure, conductivity, and ionic motion in $Na_{1+x}Zr_2Si_xP_{3-x}O_{12}$: a simulation study*, J. Phys. Chem. B 106(28) (2002), pp. 7081–7089.